Reaction Kinetics, Mechanisms and Catalysis
https://doi.org/10.1007/s11144-022-02291-x

Differently shaped Al_2O_3-based Pd catalysts loaded catalytic converter for novel non-road mobile machinery exhaust systems

Owais Al-Aqtasha[1] · Ferenc Farkas[2] · András Sápi[1] · Imre Szenti[1] · Tamás Boldizsár[1] · Kornélia B.Ábrahámné[1] · Ákos Kukovecz[1,2] · Zoltán Kónya[1,3]

Received: 2 June 2022 / Accepted: 2 September 2022

Abstract

A quick overview of the increasing pollutants worldwide shows a parallel movement toward strict legalization to limit contamination of air before it gets out of hand, however, in this paper, we are discussing a source of emissions that is yet to receive its' deserved attention rendered in non-road mobile machinery. Our proposal to solve this issue unfolds by delivering an efficient catalyst, starting by characterizing its relevant properties such as the choice of material, the shape of the catalyst, the chemical structure, and the active coating agent. So, in this sequence of experiments, we are investigating the performance of five ceramic supports impregnated with 0.1 and 0.2 wt% palladium (II). Starting by testing the samples' ability to oxidize CO in a fixed bed reactor, we will measure their performance in converting flue-gas emissions by testing the samples on a custom-designed catalytic converter connected to a dynamometer system. Following this study, we can achieve an outstanding 98% reduction in NOx and 95% reduction in CO and build a direct relation between sample properties and performance. For now, this research will be the first part of a tailored proposed solution to reduce NRMM emissions using a catalytic converter where this paper will mostly be concerned with the overall performance of the catalyst.

Keywords Flue gas treatment · NRMM · Catalytic converter · Shape designed catalysts

✉ András Sápi
sapia@chem.u-szeged.hu

[1] Department of Applied and Environmental Chemistry, Interdisciplinary Excellence Center, University of Szeged, 6720 Rerrich Béla tér 1, Szeged, Hungary

[2] Department of Technology, Faculty of Engineering, University of Szeged, H-6724 Mars tér 7, Szeged, Hungary

[3] MTA-SZTE Reaction Kinetics and Surface Chemistry Research Group, University of Szeged, 6720, Szeged, Hungary

Published online: 21 September 2022

Introduction

The increased number of pollutant sources and the lack of efficient catalytic converters made the "diesel boom" that began in the European Union in the mid-1990s most certainly provide a little climate benefit in terms of total CO2-eq emissions between 1995 and 2015 where CO_2 emissions were reported at 8395 Mt and 11,761 Mt respectively [1, 17]. Moreover, between 2008 and 2015 the worldwide production of biodiesel increased from 1.6 to 3.2 million m^3 per year [2, 18]. For that many strict regulations were applied worldwide on vehicle exhaust and various sources of emissions as the air pollutants produced contribute to a major air quality problem, arguably most important is health problems. For example, according to a large number of studies confirm that air pollution can cause a variety of diseases, including stroke, chronic obstructive pulmonary disease, trachea, bronchus, lung cancer, increased asthma, and lower respiratory infections [3, 4, 19, 20]. The European Union (EU) has set a goal of reducing emissions by 80–95 percent to be achieved by 2050 [6], with a proposal for additional emission reductions that would bring the EU to climate neutrality by 2050 [5]. this paper will be concentrating on a massively overlooked source of pollutants caused by Non-Road Mobile Machinery (NRMM), which is a transportable or mobile machine that is not intended to transport passengers or goods on roads. It also includes machines installed on passenger or transport vehicles [7, 21, 22]. According to a report published in 2017, NRMM was responsible for 15% of overall NOx emissions and 5% of total PM emissions in the European Union [8, 9]. The table below shows statistical ratios of NRMM in the London area [10]

In this study, we opted to use different types of Aluminum oxide (Al_2O_3) in the process of catalytic oxidation of flue-gas emissions for their high mechanical properties and resistance to thermal decomposition [11]. Moreover, Al_2O_3 is known for its acidity which increases the catalytic activity, furthermore, it's a non-toxic, easy-to-use, and chemically stable material [12]. Nobel metal palladium was also chosen over metal oxides as an agent because of their superior specific activity and selectivity, making them the best candidates for low-temperature complete oxidation [13]. The key property that we are most keen to address its effect on catalytic activity is the shape of the samples and the structure of their masses inside the catalytic converter since we believe that this approach will have numerous advantages over its conventional counterparts such as more rigidity and less exposure to choking and melting, the ease in adjusting catalytic converter capacity according to the engine volume, and the seamless recovery and restoration of catalysts.

In this sequence of experiments, we investigated the performance of five ceramic supports impregnated with 0.1 wt% Pd. First, we tested the samples' ability in oxidizing CO in a fixed-bed reactor and the best performing materials were further tested on a custom-designed catalytic converter connected to a dynamometer setup to measure their performance in converting flue-gas emissions. The results showed outstanding performance by the pellets and spherical shapes caused by their characteristic length and high BET surface area. This

research will be the first part of a tailored proposed solution to reduce NRMM emissions using a catalytic converter where this paper will mostly be concerned with the choice of support material, coating agent, durability, and the overall performance of the catalyst (See Table 1).

Experimental methods & materials

Sample properties

As the reaction of oxidation is exothermic, catalyst shape and structure nature play an important role in facilitating the heat release from particle to gas, this assumption can be approved by monitoring the temperature of the exhaust outlet gas. To regard the differences in sample geometry, we need to determine most of their physical properties such as the characteristic length and void fraction for better comparison. We can determine these values using the following equations and substituting the appropriate values according to the shape geometry.

$$\text{Characteristic length} = \frac{\text{surface area}}{\text{volume}}$$

$$Voidfraction = \frac{empty\ tube\ volume}{total\ tube\ volume}$$

Below are the basic proprieties summed up in Table 2 showing the BET, characteristic length, and void fractions of the samples that may affect the performance in converting flue-gas emissions.

Materials

Palladium (II) acetate (Pd(OCOCH3)2); ≥ 97%) was manufactured by Sigma Aldrich. The raw materials used for the production of the porcelain mass were obtained from the following companies: Alumina (Al2O3, ≥ 95%) was manufactured by SILKEM Hungary Ltd.; talc (Mg3(Si4O10(OH)2), ≥ 85%) was traded by Imerys

Table 1 Data on the flue gas emitted by NRMM in the London area, and their ratio to road traffic emissions

Pollutant		2010	2013	2016
CO2	tons/year	187.126	179.956	200.388
	NRMM to Road traffic emission ratio	27%	30%	29%
NOX	tons/year	5833.2	3967.5	3214.2
	NRMM to Road traffic emission ratio	51.2%	51.5%	48%

Table 2 Basic properties of the ceramic samples containing their mass, BET surface area, characteristic length, and void fraction

Shape	Mass/pcs	BET surface area (m^2/g)	Surface area to volume ratio for a 400–500 mg of catalyst (mm^{-1})	Void fraction
Cylindrical/no holes 0.1wt% Pd	0.47 g	1–2	0.8	0.969
Cylindrical/one hole 0.1wt% Pd	0.49 g	1–2	0.88	0.971
Cylindrical/4 holes 0.1wt% Pd	0.46 g	1–2	1.16	0.979
Pellets 1/8″ 0.1wt% Pd	0.07 g	200	6.75	0.972
Spherical 0.1wt% Pd	0.09 g	326	10.4	0.984

Refractory Manufacturer Ltd. Hungary and clay (Al2O32SiO2 + 2H2O, clay minerals ≥ 85%) was manufactured by Keraclay Plc. Czech Republic.

Ceramic support preparation

Using the appropriate quantities of raw materials, a dense ceramic mass was prepared by adding water to it, which was homogenized several times so the clay components were enough time to unfold. After approximately one week of daily homogenization process, when the moisture content of the ceramic mass reached 22–25% we started to produce the three types of cylindrical ceramic bodies with the vacuum press extrusion method. The drying process took two weeks in the case of this type of extruded sample, after that they were heat-treated two times at elevated temperatures (900–1250 °C).

The ceramic bodies including the cylinders without holes and the one-hole and four-hole ones were all made of a hard porcelain ceramic mass, with the following typical oxide composition (64,21% SiO2; 20,98% Al2O3; 2,08% Fe2O3; 1,85% TiO2; 1,75% Na2O; 1,69% K2O; 0,90% CaO; 0,35% MgO; 6,19% LOI = Loss on Ignition).

As for the spherical-shaped and the Pellets catalysts they both are Gamma-Alumina, which means both of them were annealed below 900–1000 °C in their fabrication process with the following approximate chemical composition for spheres (46% SiO_2, 39% Al_2O_3, and 14% H_2O).

Catalyst sample preparation

All catalyst samples were prepared using the wet impregnation method to create a wash-coat covering the ceramic support. Firstly, the impregnating solution is prepared by dissolving palladium (II) acetate in Acetone solvent using an ultrasonic sonication bath for 5 min, the exact amount of dissolved palladium (II) salt was proportional to the mass of the ceramic support that the resulted sample was 0.1 *wt*% of Pd for 125 g of ceramic support. Once the solution was ready to use a dropper was used to impregnate the ceramic support with the solution. Afterward, it was dried

in an 80 °C oven for 1 h, and the same process was repeated until all the solution is completely absorbed by the ceramic sample.

Characterization methods

CO oxidation

first, we started by testing the catalyst activity which was determined using Fixed-bed connected to a gas chromatography (GC) type Hewlett Packard 5890 Series II. A constant mass of 450–500 mg of solid catalyst samples was placed in the middle region of a 1 mm wall thickness, 8 mm internal diameter, 200 mm long quartz tube that was inserted vertically into a tube furnace during the measurements. Before initiating the measurement, the samples were oxidized and then reduced. During the oxidation, the sample was purged with pure O2 gas for 30 min at 300 °C. After oxidation, the system was purged for 5 min with pure Argon. Following oxidative pretreatment and argon purging, the samples were reduced. During the reduction, the sample was purged with pure H_2 for 30 min at 300 °C to remove unwanted surface poisons. Then, the entire system was purged with Argon for 5 min. Following the pretreatment of the catalyst samples, our system was cooled back to 60 °C, and measurements were taken using a CO–O_2–Ar reaction gas mixture at seven different measuring points ranging from 60 to 200 °C. Our reaction gas mixture flow rate was 4–10–46 mL/min during the O_2 rich measurement condition and 10–4–46 mL/min during the CO rich measurement condition, respectively. The thermal conductivity detector (TCD) provided the signal based on the different thermal conductivity of the components.

X-ray diffraction (XRD)

The composition of our samples was determined using a Rigaku MiniFlex II X-ray diffractometer. For the maximum possible resolution, the samples were evaluated at a measurement speed of 2°/min. Cu K anode X-ray source was adopted for the measurements.

Flue-gas conversion

The equipment consists of two main systems, a controlled flue-gas emission source, and a gas analyzer. The first includes a mobile design measuring table with a galvanized surface on wheels and a damage-prevention frame. The load unit used is a 3-phase asynchronous electric motor, which also performs as the starter of the internal combustion engine. The engine used is a HONDA GX390, a 4-stroke single-cylinder OHV petroleum engine with a net power of 8.7 KW. The static working point setting or the control of the complete measuring cycle can be performed utilizing the ENERGOPOWER (Telj-4) measuring software, which also controls the operation of large braking systems. And the second is gas analyzer probs of the type testo

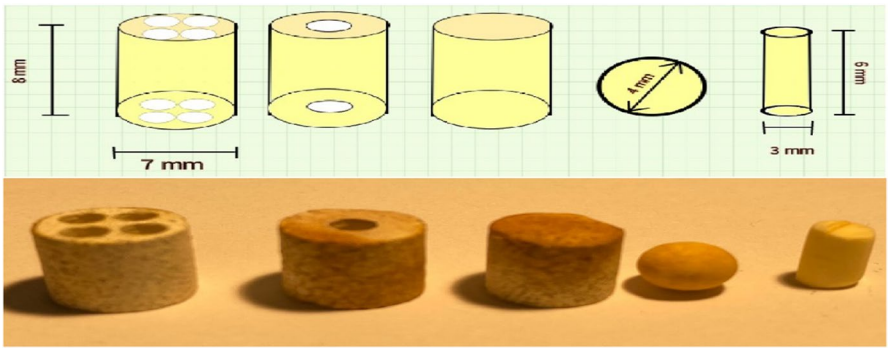

Fig. 1 the dimensions and shape of the five different samples used in the experiments

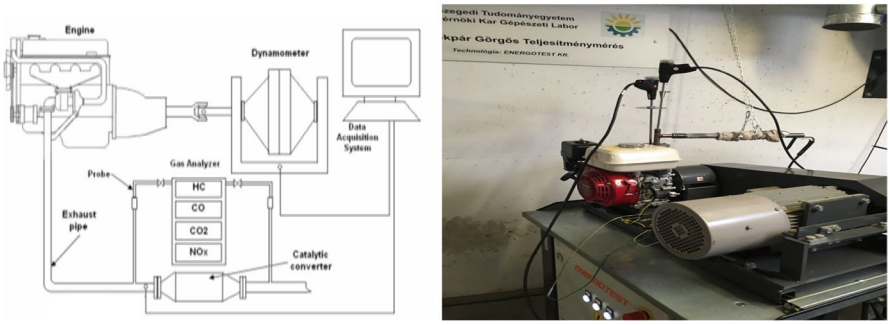

Fig. 2 Schematic representation and a real photo of the flue-gas conversion characterization setup

350 that were installed before and after the catalyst sample. The testo 350 emission analyzers can measure a wide range of flue gas components, including carbon monoxide (CO), carbon dioxide (CO_2), nitrogen oxides (NOX), and sulfur dioxide (SO_2) as well as pressure and temperature differences. Gas analyzers are connected to a computer and their data are collected through Testo Easy Emission software. The measurements were done at 3 different points 1500 rpm, 2500 rpm, and 3500 rpm. The catalytic converter chamber was designed to fit our catalyst samples and was attached to the engine's exhaust outlet (See Figs. 1 and 2).

Coke resistant tests by Transmission Electron Microscopy

This characterization was carried out to identify the pellets sample's ability to resist coke formation, which reveals the direction of the pellets sample's capacity to perform consistently for long periods. The experiment was held under 1500 rpm and 1 N m at which emissions are typically high, the experiment was repeated three times lasting 1 h each, and the mass of the catalyst used was 63 g. Fig. 3 below

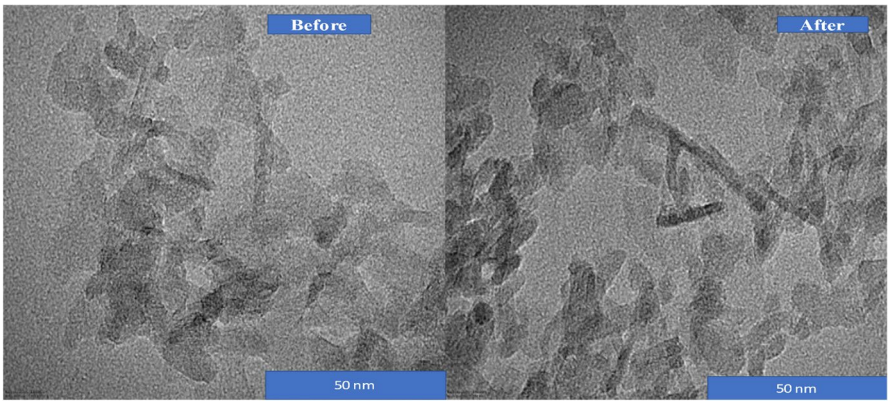

Fig. 3 TEM image of pellet sample before and after performing inside a catalytic converter for three hours

shows the TEM images of the sample before and after performing in the catalytic converter showing no signs of coke formation.

Result and discussion

X-ray diffractogram (XRD)

XRD patterns of Pd/ceramic support were obtained in the range of 10 to 90 2θ and illustrated in Fig. 4. The chemical composition of the ceramic support showed mainly hexagonal α-aluminum oxide (α-Al_2O_3) for the cylindrical shape samples,

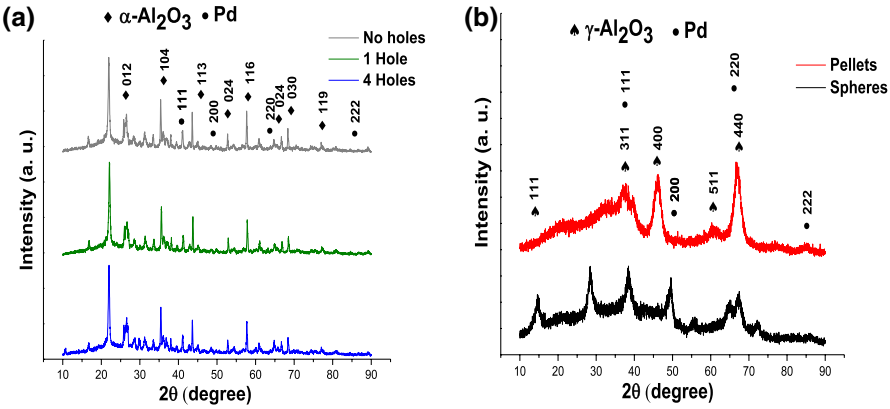

Fig. 4 XRD patterns of the ceramic support powders containing 0.1wt% Pd, where Panel a shows the peeks of alpha Aluminum oxide as well as Pd peeks, and Panel b represents the peeks of gamma Aluminum oxide and Pd

and mainly cubic γ-aluminum oxide (γ- Al_2O_3) for the pellets and spheres, where all the samples contained 0.1 wt% Pd.

It can be observed from the XRD results that the peaks of the first three samples (a.) correspond to alpha-alumina and are crystalline, while the next 2 samples (b.) are gamma-alumina and are rather amorphous.

Typical α-Al_2O_3 peaks can be seen on the left side XRD figure at 25 (012); 35 (104); 44 (113); 53 (024); 57 (116); 66 (024); 68 (030) and 77 (119) 2θ degrees, which correspond to corundum.

Characteristic γ-Al_2O_3 peaks can be observed on the right side XRD figure at 15 (111); 37 (311); 46 (400); 60 (511) and 67 (440) 2θ degrees.

Pd peaks can be seen on both XRD figures at 40 (111); 47 (200); 68 (220) and 86 (222) 2θ degrees.

CO oxidation measurements

CO oxidation measurements were held to select the most appropriate catalyst to perform heterogeneous catalytic measurement inside the catalytic converter. The experiments were executed using a fixed bed connected to a gas chromatograph, in order to imitate the lean and rich conditions occurring inside an internal combustion engine, which generally refers to the ratio between air and fuel in the combustion chamber, the experiments were held under two different conditions: (a) the first condition represented an oxygen-rich case at which O_2 gas flow was 2.5 times higher

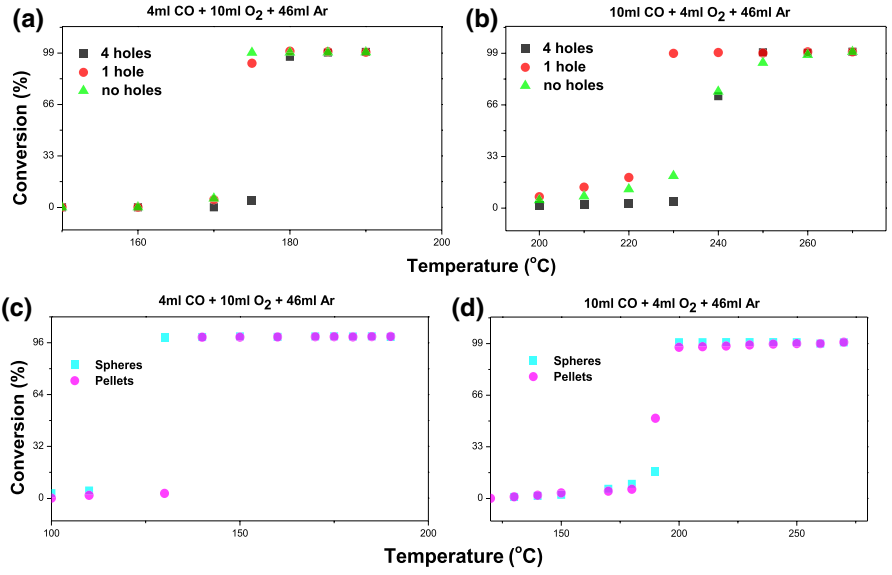

Fig. 5 CO conversion as a function of temperature for five different shapes of ceramic samples, where all samples contain 0.1 wt% Pd. Panels a. and b show the performance of no holes, one hole, and four holes samples at low temperature and high temperature respectively. Panels c and d. show the performance of spheres and pellets samples at low and high temperatures respectively

than CO flow, while (b) the second condition represented an oxygen-deficient case, where the CO gas flow was 2.5 times bigger than O_2 flow. From Fig. 5a related to the GC test, we noticed that the three alpha-alumina catalysts gave very similar activity under the O_2 rich condition where all samples reached complete oxidation at 175–178 °C.

In Fig. 5b the one-hole catalyst has a slightly better performance than the 4-holes and no-holes catalysts since it has a two times bigger diameter. The bigger diameter of the hole affects the diffusion through the catalyst instead of increasing the contact surface area. Changing the condition to lean reduced the activity of catalysts, where reaching complete oxidation was around 230 °C for the one-hole and 250 °C for the rest, this decrease in activity is due to the low O_2 concentration needed to oxidize CO. In Fig. 5c, we can observe the conversion of gamma-alumina for both pellets and spheres, starting at lower temperatures and reaching complete oxidation significantly faster than the alpha-alumina, this performance is probably due to their nature of amorphous structure and their orders of magnitude larger BET surface area, as well as the similar void fraction values make this assumption more likely. In Fig. 5d we can observe another significantly better performance of the pellets and spheres under lean conditions where all samples reached complete oxidation at 190 °C. To show these results in perspective compared with CO oxidation experiments Fukun et. al. reported a start of conversion at 150 °C reaching complete oxidation at 200 °C for 0.1 wt% Pd loading and a slightly earlier conversion of 0.3, 0.5, and 0.8 wt% Pd loading all supported UiO-66, the experiments were held under the rich condition with 1:20 CO to O_2 ratio [14]. Xiaodong et. al. reported a start of CO oxidation at 150 °C and a 20% conversion at 200 °C for CeO_2, where CuCeO-IMP started converting at 100 °C reaching complete oxidation at 200 °C, also 1:20 CO to O_2 gas mixture ratio was utilized for this test [15]. In a more relative experiment, Nur Izwanne et. al. reported a start of conversion at 150 °C reaching complete oxidation at 200 °C for Gamma-Al_2O_3 loaded with 3, 5, 8, and 10 wt% of Pd, the gas mixture ratio was 1:2 CO to O_2 [16]. A great distinction can be seen in the performance of our samples and the compared counterparts, showing a significantly higher activity both in the early start of conversion as well as at complete oxidation, furthermore even at low O_2 concentrations both alpha-alumina and gamma-alumina were rendered superior. Additionally [24–27] carried out a similar fixed bed reactor measurement.

Flue-gas conversion

similar to the CO oxidation tests we used a constant mass of catalyst, for that we prepared 63 g of each of the five samples with the wet impregnation method, moreover, we increased the loading of Pd to 0.2 wt% instead of 0.1 wt% to withstand a large amount of flue-gas emitted by the 8.7 KW engine, and lastly, we pretreated each sample and reduced them at 800 °C for 12 h before testing them. The experiments were carried out for approximately 1 h per sample at three points (1500 rpm, 2500 rpm, and 3500 rpm) to ensure stable combustion leading to stable results. Reduction percentages of NO_x and CO for the 5 samples are shown in Fig. 6. It

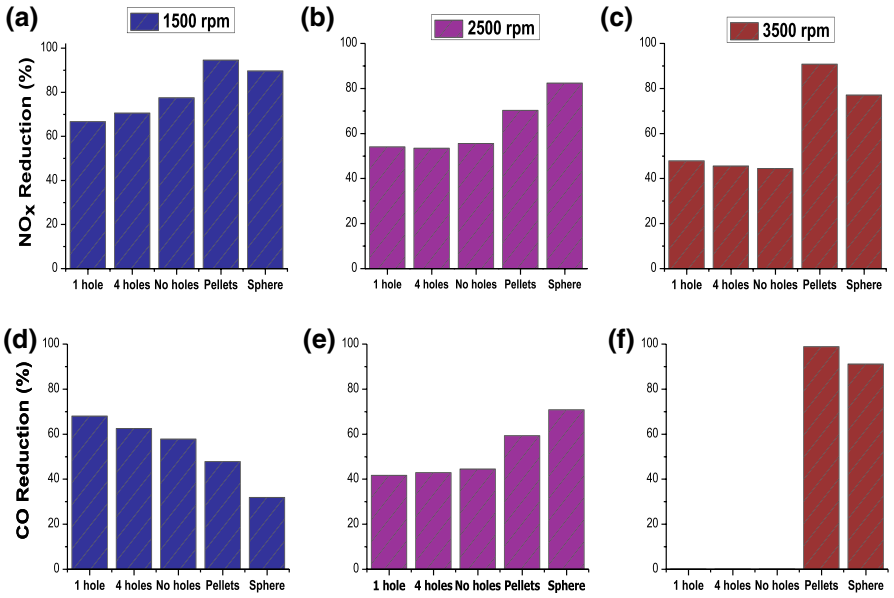

Fig. 6 Performance of the five ceramic samples in reducing NOx and CO at three different engine speed points (1500 rpm, 2500 rpm, and 3500 rpm)

is worth mentioning that with the increase in rpm of the engine, the flow volume, speed, and temperature will also increase as can be seen in the direct relation in the following equation [23]:

$$V_{Exhaust} = \frac{T_{Exhaust}}{300} \times V_{Intake}$$

$V_{Exhaust}$ = Exhaust volume flow rate, $T_{Exhaust}$ = Temperature of exhaust gas in kelvin, V_{Intake} = Intake volume flow rate.

And for a 4-stroke engine the Intake volume is as follows:

$$V_{Intake} = \left(V_{stroke} \times \frac{N}{2}\right) \times \mu_{volumetric}$$

V_{stroke} = Swept volume of the engine, $\mu_{volumetric}$ = volumetric efficiency of the engine, N = RPM of the crankshaft.

In Fig. 6a all samples showed excellent catalytic activity in oxidizing NO_x at which both the pellets and spheres showed better performance as was expected indicated by their activity in the fixed-bed reactor, moving forward pellets and spheres continued their preferable performance at higher flow, speed, and temperature at 2500 rpm and 3500 rpm illustrated in Figs. 6b and 6c. On the other hand, Figs. 6d, 6e, and 6f show the reduction of CO using the five different samples, in Fig. 6d. the cylindrical samples had a slightly better performance at a low flow speed which may occur because of their higher void fraction at this mass, leaving

more time for the flue gas to diffuse throw the catalyst and increasing the contact surface area. However, the pellets and the spheres samples gained back the edge regarding the catalytic activity at 2500 rpm and 3500 rpm where the flow, speed, and temperature of the flue gas increased as shown in Figs. 6e and 6f. one explanation for this performance presented by the pellets and spheres samples is their amorphous nature and high BET surface area, moreover, their activity in the fixed bed reactor is also corresponding to their performance in the catalytic converter. As for the overall performance comparison it's very much dependent on the application, on one side the pellet-shaped catalyst showed the best conversion of NO_x and CO at 1500 rpm and 3500 rpm, so it's a favorable option for application in which engines runs more at these speeds, on the other hand, the results suggest that the spherical catalyst will have higher activity in the applications at which engines runs more around 2500 rpm, lastly if the engine is continually changing speeds then pellets are once again the favorites as they cover more speed range.

By comparing these findings with industrial catalytic converters, we find our sample superior in converting emissions in different regards, most notable are the conversion at low temperatures (typically temp. at 1500 rpm is around 190 °C ranging to 500 °C at 3500 rpm) and the amount of conversion. For example, most engineering books present the industrial catalytic converter's ability to oxidize CO as follows, a typical 90 percent oxidation of CO occurs at about 300 °C, and the conversion efficiency falls to zero at about 150 °C to 200 °C the same percentages also apply to NO_x [28]. Moreover, in a modern article, we see a conversion of CO ranging between 30%—80% at different RPMs for industrial catalytic converters [29] and an average of 52% reduction of co in some other experiments [30].

Conclusion

The geometric features of the five ceramic supports inspired a reliable and easy-to-install solution for the reduction of the emissions produced by NRMM, where a fabricated catalytic converter chamber and an adequate amount of catalyst are enough to decrease pollution drastically. This case can also be profiled to suit NRMMs according to their features. We have shown that by wet impregnation method we were able to wash-coat our samples with 0.1 and 0.2 wt% Palladium (II)-acetate, and the carried-out tests indicated that Pd supported Aluminum-oxide catalysts are promising for efficient CO oxidation and selective oxidation of flue gas components. The exact property or set of properties that gave the spherical and the pellet-shaped catalysts their edge over their counterparts can't be defined by our experiments, however, the fixed bed reactor measurements strongly suggested that amorphous structure and the order of magnitude larger BET surface area were the only significant variables hence the better performance is most likely regards to them. Lastly, the overall performance comparison recommended the pellets catalyst for the applications where the engine run more around 3500 rpm and the spherical catalysts for the application at which the engine run more around 2500 rpm.

Acknowledgements Project no. TKP2021-NVA-19 has been implemented with the support provided by the Ministry of Innovation and Technology of Hungary from the National Research, Development and Innovation Fund, financed under the TKP2021-NVA funding scheme. AS gratefully acknowledges the support of the Bolyai Janos Research Fellowship of the Hungarian Academy of Science and the "UNKP-21-5-SZTE-586" New National Excellence Program as well as the funding provided by the Indo-Hungarian TÉT project (2019-2.1.13-TÉT_IN-2020-00015) of the Ministry for Innovation and Technology from the source of the National Research, Development and Innovation Fund. The Ministry of Human Capacities through the EFOP-3.6.1-16-2016-00014 project and the 20391-3/2018/FEKUSTRAT are acknowledged. ZK is grateful for K_21 138714 and SNN_135918 project for the Hungarian National Research, Development and Innovation Office.

References

1. Helmers E, Leitão J, Tietge U, Butler T (2019) CO2-equivalent emissions from European passenger vehicles in the years 1995–2015 based on real-world use: assessing the climate benefit of the European "diesel boom." Atmos Environ 198:122–132
2. Schünemann S, Schüth F, Tüysüz H (2017) Selective glycerol oxidation over ordered mesoporous copper aluminum oxide catalysts. Catal Sci Technol 7(23):5614–5624
3. Kagawa J (2002) Health effects of diesel exhaust emissions—a mixture of air pollutants of worldwide concern. Toxicology 181:349–353
4. Burr ML, Karani G, Davies B, Holmes BA, Williams KL (2004) Effects on respiratory health of a reduction in air pollution from vehicle exhaust emissions. Occup Environ Med 61(3):212–218
5. European Commission State of the Union: Commission Raises Climate Ambition. Available online: https://ec.europa.eu/commission/presscorner/detail/en/IP_20_1599. European Commission - Press release Brussels, 17 September 2020
6. European Commission. A Roadmap for Moving to a Competitive Low Carbon Economy in 2050; European Commission: Brussels, Belgium, 2011. http://eur-lex.europa.eu/LexUriServ/LexUriServ.do?uri=COM:2011:0112:FIN:EN:PDF
7. EU. Regulation 2016/1628 on Requirements Relating to Gaseous and Particulate Pollutant Emission Limits and Type-Approval for Internal Combustion Engines for Non-Road Mobile Machinery, Amending Regulations (EU) No. 1024/2012 and (EU) No. 167/2013, and Amending and Repealing Directive 97/68/EC (Text with EEA Relevance); European Union: Brussels, Belgium, 2016. Official Journal of the European Union. https://eur-lex.europa.eu/legal-content/EN/TXT/?uri=celex:32016R1628
8. European Comission. Impact Assessment Accompanying the Document "Review of Directive 97/68/EC on Emissions from Engines in Non-Road Mobile Machinery in View of Establishing a New Legislative Instrument"; European Comission: Brussels, Belgium. https://eur-lex.europa.eu/legal-content/PT/ALL/?uri=CELEX:52014SC0282
9. Poulsen TS (2017) Market analysis for non-roadmobilemachinery sector. Scandinavian GPP Alliance, Copenhagen, p 40
10. Lončarević Š, Ilinčić P, Šagi G, Lulić Z (2022) Problems and directions in creating a national non-road mobile machinery emission inventory: a critical review. Sustainability 14(6):3471
11. Hami HK, Abbas RF, Eltayef EM, Mahdi NI (2020) Applications of aluminum oxide and nano aluminum oxide as adsorbents. Samarra J Pure Appl Sci 2(2):19–32
12. Sung DM, Kim YH, Park ED, Yie JE (2010) Correlation between acidity and catalytic activity for the methanol dehydration over various aluminum oxides. Res Chem Intermed 36(6):653–660
13. Huang S, Zhang C, He H (2008) Complete oxidation of o-xylene over Pd/Al2O3 catalyst at low temperature. Catal Today 139(1–2):15–23
14. Bi F, Zhang X, Du Q, Yue K, Wang R, Li F, Huang Y (2021) Influence of pretreatment conditions on low-temperature CO oxidation over Pd supported UiO-66 catalysts. Mol Catal 509:111633
15. Zhang X, Zhang X, Song L, Hou F, Yang Y, Wang Y, Liu N (2018) Enhanced catalytic performance for CO oxidation and preferential CO oxidation over CuO/CeO2 catalysts synthesized from metal organic framework: effects of preparation methods. Int J Hydrogen Energy 43(39):18279–18288

16. Mahyon NI, Li T, Martinez-Botas R, Wu Z, Li K (2019) A new hollow fibre catalytic converter design for sustainable automotive emissions control. Catal Commun 120:86–90
17. Trotta G (2019) Assessing energy efficiency improvements, energy dependence, and CO2 emissions in the European Union using a decomposition method. Energ Effi 12(7):1873–1890
18. Hekkert MP, Van den Reek J, Worrell E, Turkenburg WC (2002) The impact of material efficient end-use technologies on paper use and carbon emissions. Resour Conserv Recycl 36(3):241–266
19. Quam VG, Rocklöv J, Quam M, Lucas RA (2017) Assessing greenhouse gas emissions and health co-benefits: a structured review of lifestyle-related climate change mitigation strategies. Int J Environ Res Public Health 14(5):468
20. Guerra G, Lemma A, Lerda D, Martines C, Salvi G, Tamponi M (1995) Benzene emissions from motor vehicle traffic in the urban area of Milan: hypothesis of health impact assessment. Atmos Environ 29(23):3559–3569
21. Lindgren M (2005) A transient fuel consumption model for non-road mobile machinery. Biosys Eng 91(2):139–147
22. Lindgren M (2007) A methodology for estimating annual fuel consumption and emissions from non-road mobile machinery-annual emissions from the non-road mobile machinery sector in Sweden for year 2006. Research Organizations: Swedish Univ. of Agricultural Sciences, Uppsala (SE). Dept. of Biometry and Engineering. http://publikationer.slu.se/Filer/Rapport_2007_01.pdf
23. González NF, Kindelán JC, Martí JML (2016) Methodology for instantaneous average exhaust gas mass flow rate measurement. Flow Meas Instrum 49:52–62
24. Hoebink JHBJ, Nievergeld AJL, Marin GB (1999) CO oxidation in a fixed bed reactor with high-frequency cycling of the feed. Chem Eng Sci 54(20):4459–4468
25. Wicke E, Onken HU (1988) Periodicity and chaos in a catalytic packed bed reactor for CO oxidation. Chem Eng Sci 43(8):2289–2294
26. Wicke E, Onken HU (1986) Statistical fluctuations of conversion and temperature in an adiabatic fixed-bed reactor for CO oxidation. Chem Eng Sci 41(6):1681–1687
27. Zhang H, Hu X (2004) Catalytic oxidation of carbon monoxide in a fixed bed reactor. Sep Purif Technol 34(1–3):105–108
28. Brian E (1998) MiltonChapter 8 Control Technologies. In: Engines S (ed) : Eran Sher Handbook of Air Pollution From Internal Combustion Engines. Elsevier, amsterdam
29. Mohiuddin, A. K. M., & Nurhafez, M. Analysis and comparison of performance characteristics of catalytic converters.
30. Warju, W., Ariyanto, S. R., Nugraha, A. S., & Pratama, M. Y. 2021. The Effectiveness of the Brass Based Catalytic Converter to Reduce Exhaust Gas Emissions from Four-stroke Motorcycle Engines. In International Joint Conference on Science and Engineering 2021. Atlantis Press.